

Quasistatic stick-slip of a dislocation core and the Frenkel-Kontorova chain

Mishreyee Bhattacharya,^{1,*} Amlan Dutta,² and Parthasarathi Barat¹

¹Variable Energy Cyclotron Centre, 1/AF Bidhannagar, Kolkata 700064, India

²Department of Metallurgical and Materials Engineering, Jadavpur University, Kolkata 700 032, India

(Received 23 April 2013; published 24 June 2013)

Stick-slip phenomenon is generally associated with a wide range of dynamical systems. Here we report a unique quasistatic form of the stick-slip characterized in terms of bursts in structural relaxation. This is demonstrated for the case of a dislocation core and its one-dimensional representation, namely, the Frenkel-Kontorova chain. The correspondence between these two is also established through the technique of dimensionality reduction.

DOI: [10.1103/PhysRevB.87.214107](https://doi.org/10.1103/PhysRevB.87.214107)

PACS number(s): 61.72.Lk, 02.70.Ns, 45.05.+x

I. INTRODUCTION

Many processes proceed through the modality of stick-slip,^{1–7} where one or more measurable parameters exhibit jerky dynamics. Events like avalanches and stick-slip are commonly associated with nonlinear systems, and hence, the celebrated Frenkel-Kontorova (FK) model,^{8,9} which is a simple one-dimensional system incorporating discreteness and nonlinearity, is often studied to understand such events.^{10–12} Nevertheless, such phenomena are always viewed in perspective of dynamics of the systems, whereas their quasistatic responses remain obscure.

During a quasistatic process, a system moves from one state to another such that it is always at the local ground state along the path of transition. For instance, in order to measure the Peierls barrier¹³ for a dislocation, which is defined at $T = 0$ K, atomistic simulations^{14–16} have been performed to obtain the ground state evolution of the dislocation core as it quasistatically moves from one Peierls valley to another. Similar to the existence of a critical Peierls stress for a dislocation, the FK chain, which was originally envisaged⁸ to represent the dislocation core as a kink in the chain, shows the existence of a threshold force required¹⁷ to move the kink. Thus, the FK model thematically depicts the mechanism of crossing the Peierls barrier in perspective of discreteness and nonlinearity intrinsic to the lattice. Nevertheless, it is unrevealed whether this simplified model is capable of providing finer details of the process. A closer look into this issue is worthwhile as it would not only highlight the extent of resemblance between the realistic physical system and the representative model, but also enable us to extend the applicability of the model to explore quasistatic evolution of the system. In this paper, we study the molecular statics simulation of forcing a dislocation core out of its Peierls valley to obtain the atomic trajectories at sub-Burgers vector resolution. Interestingly, the simulations reveal the occurrence of intermittent relaxation bursts at such fine scale. Aiming to unfold the underlying mechanism, we apply the appropriate boundary conditions to a simple one-dimensional FK chain to let it mimic the boundary conditions used in the atomistic simulation. Even though the FK model is regarded merely as a conceptual tool, it also exhibits the abrupt bursts of structural relaxation, similar to the dislocation core. In what follows, we shall argue that such a striking feature can be perceived as the unique quasistatic counterpart of the stick-slip dynamics, which has not been explored so far. In addition, the technique

of principal component analysis (PCA)¹⁸ has been used in an innovative way to establish the correspondence between a real physical system and its ideal model of lower dimensionality.

II. ATOMISTIC SIMULATIONS: OBSERVATION OF STICK-SLIP

The Peierls stresses have been computed here¹⁹ for the four metals, molybdenum, iron, aluminium and copper, where the simulation scheme is akin to that used in the earlier measurements.^{14,16} An edge dislocation is introduced in a slab of finite thickness with periodic boundaries along the directions of dislocation line and Burgers vector. The x , y , and z dimensions of the bcc simulation cells are $90.5a\langle 111 \rangle/2$, $40a\langle \bar{1}01 \rangle$, and $5a\langle 1\bar{2}1 \rangle$, where a is the lattice constant. The Burgers vectors and the dislocation lines are along the x and z directions, respectively [see the inset of Fig. 1(a)]. Corresponding cell dimensions for the fcc systems are $90.5a\langle 101 \rangle/2 \times 20a\langle \bar{1}11 \rangle \times 5a\langle 12\bar{1} \rangle$, where the perfect dislocations splits into Schockley partials on account of the Frank's criterion.²⁰ Shear strain in the system is increased in small steps by tilting the vertical boundary of the simulation cell. At each step, the system is relaxed to the minimum energy configuration using the conjugate gradient method,¹⁴ while the top and bottom surfaces are kept fixed during the relaxation. The potential energy of the system is recorded and the crossover of the dislocation core to the next Peierls valley is marked by a drastic drop in the total potential energy profile. Detailed analysis of the simulation output involves the region only up to the crossover points, as shown in Fig. 1(a). The dislocation core atoms are identified by using suitable centrosymmetric deviation parameter (CSD) windows.¹⁴ For bcc Mo and Fe, the CSD window of range $1.4\text{--}10 \text{ \AA}^2$ has been used, while the ranges $3\text{--}20 \text{ \AA}^2$ and $3\text{--}16 \text{ \AA}^2$ are employed for Al and Cu, respectively.²¹

As the process of applying incremental shear strain is followed by relaxation, the atomic structure tends to reconfigure so that the potential energy of the system is minimized. The core structure can be specified by a set of n_c vectors, say $\{\mathbf{r}_i\}$ ($i = 1, 2, \dots, n_c$), where n_c is the number of atoms in the dislocation core. We can now quantify the extent of aggregate core displacement at the n th step of incremental shear strain with respect to the previous step as $\Delta = \sqrt{\sum_{i=1}^{n_c} |\mathbf{r}_i(n) - \mathbf{r}_i(n-1)|^2}$. These differential displacements of the dislocation cores are plotted with the shear strains in

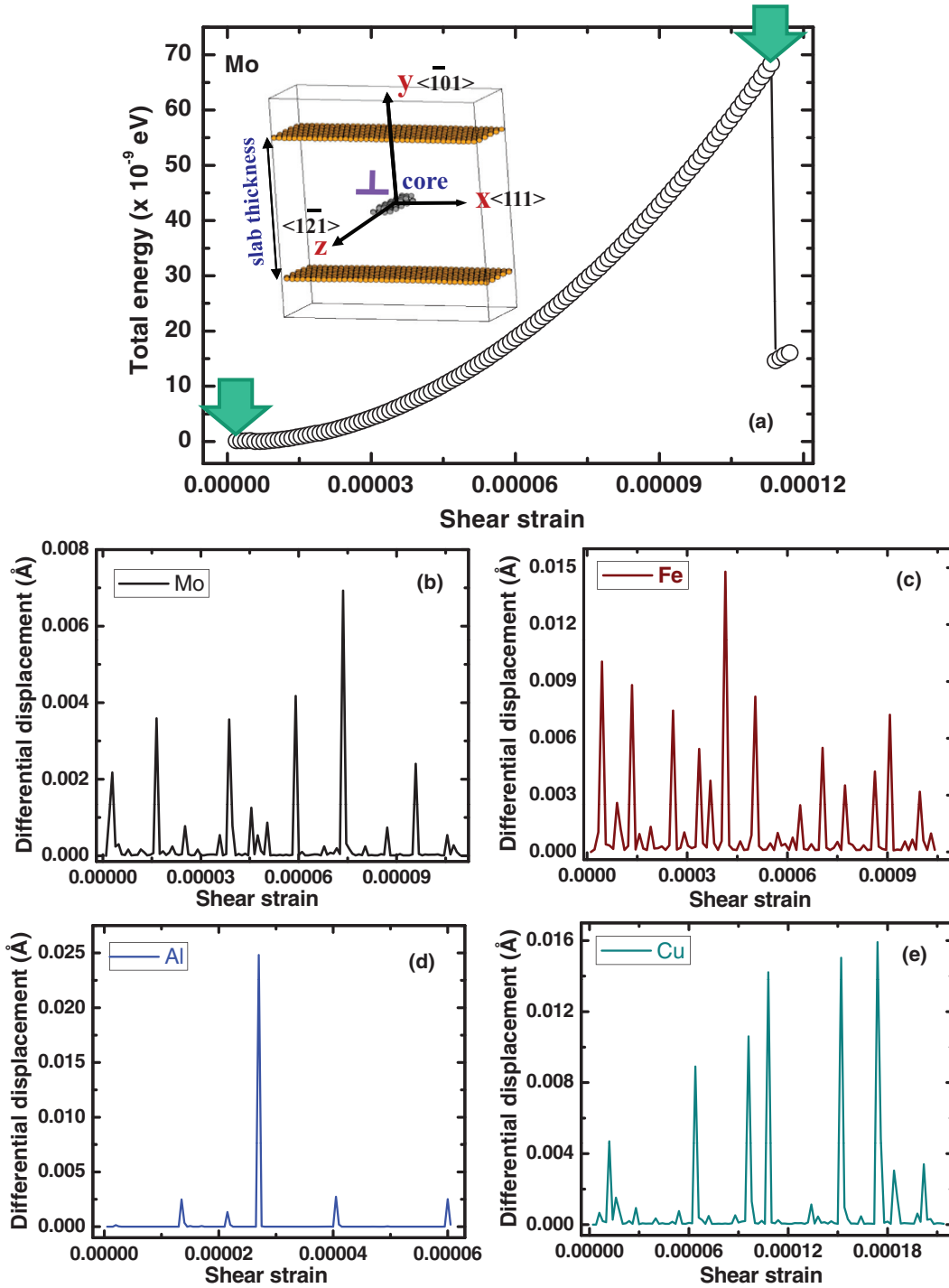


FIG. 1. (Color online) (a) Rise in potential energy of the Mo crystal with a typical simulation cell in the inset. Note the sudden drop marking the instant of crossover to the adjacent Peierls valley. The differential displacement profiles for the dislocation core atoms are shown in (b) Mo, (c) Fe, (d) Al, and (e) Cu.

Figs. 1(b)–1(e). Surprisingly, one can identify the intermittent relaxation bursts characterized by narrow peaks in the profiles. Obviously, a small value of Δ means that $\mathbf{r}_i(n) \approx \mathbf{r}_i(n - 1)$, implying only a small structural change in the dislocation core from the previous step of applied strain, whereas a large value is indicative of drastic structural rearrangement. This proves that instead of exhibiting a continuous response to the incremental strain, the dislocation core structure remains al-

most locked in between two successive bursts. This quasistatic phenomenon is apparently analogous to the stick and slip states of dynamic variables in many physical processes of interest.

III. STICK-SLIP IN THE FRENKEL-KONTOROVA MODEL

In this study, the bcc metals Mo and Fe are simulated using the modified Finnis-Sinclair interatomic potential,²²

whereas the glue potential²³ and an embedded atom model²⁴ are used for Al and Cu, respectively. In spite of a variety of potentials used in these computations, the relaxation bursts can be observed in all the studied systems. This suggests that the origin of these bursts lies rather in a more fundamental physical phenomenon than in the complexities of the potential models employed in the simulations. In this context, the possibility of closely investigating the FK model arises as it reflects the basic features of a dislocation core, namely, the nonlinear nature of interactions and discreteness of the lattice. The FK model consists of a linear chain of particles connected by springs and placed over a substrate potential. In its most elementary form, the springs are assumed to be Hookean, while a sinusoidal substrate potential is considered. Thus, the potential energy of a finite FK chain with N connected particles is given by $U = \sum_{i=1}^N [\frac{\kappa}{2}(x_{i+1} - x_i - l)^2 + E(1 - \cos \frac{2\pi x_i}{b})]$, where the first term denotes the harmonic spring potential with x_i the position of the i th particle, l the equilibrium length of each spring, and κ the spring constant. The second term represents the substrate potential where b and E are the periodicity and magnitude of the potential, respectively. Here we assume the natural length of the springs connecting the adjacent atoms to be equal to the periodicity of the substrate potential (i.e., $l = b = 1$ arb. unit). At this point, it should be noted that despite its success in demonstrating the origin of the Peierls barrier, the FK chain does not exhibit a direct correspondence to the dislocation core in all aspects. For instance, the long range interactions between two dislocations²⁰ is in clear contrast to the exponential short range kink-kink interactions in the FK chain.⁹ Thus, a judicious choice of boundary conditions and parameters of the FK chain is necessary so that the system can distinctly show the features of interest. In the atomistic simulations, the top and bottom surfaces of the crystalline slabs were kept fixed during the relaxation process so that the system could not revert back to the previous state of shear strain. To implement this on our FK chain, we fix both of its ends, thereby yielding a fixed length and fixed density condition. We accommodate N particles in N_v valleys so that the coverage parameter N/N_v is close to $\sim \frac{3}{2}$ to approximately resemble the local coverage due to the extra half-plane of atoms at the core of an edge dislocation. The chain is gradually shifted in small steps of δ and relaxed after each shift keeping the first and the last particles rigid during the relaxation process. Hence, the net shift of the chain at the n th step can be represented by the coordinates of the fixed end particle as $\Phi = x_1 = n\delta$, where the incremental shift (δ) should have been infinitesimally small for the ideal quasistatic process. However, due to the tradeoff between computational time and resolution, a small value of $\delta = 10^{-2}$ (arb. units) is chosen and found to be sufficient to produce the requisite spatial resolution. Moreover, in the present case of smooth periodic substrate potential, the simple steepest-descent algorithm¹⁴ reasonably yields the relaxed states.

The differential displacements (Δ) are now computed for the particles of the FK chain for different E/κ ranging from 0.01 to 0.1. Figure 2(a) shows the differential displacement for $E/\kappa = 0.01$ as a function of the shift Φ , imparted to the chain where a continuous wavy nature can be observed (see the supplementary movie clip.²⁵) In addition, the change in the

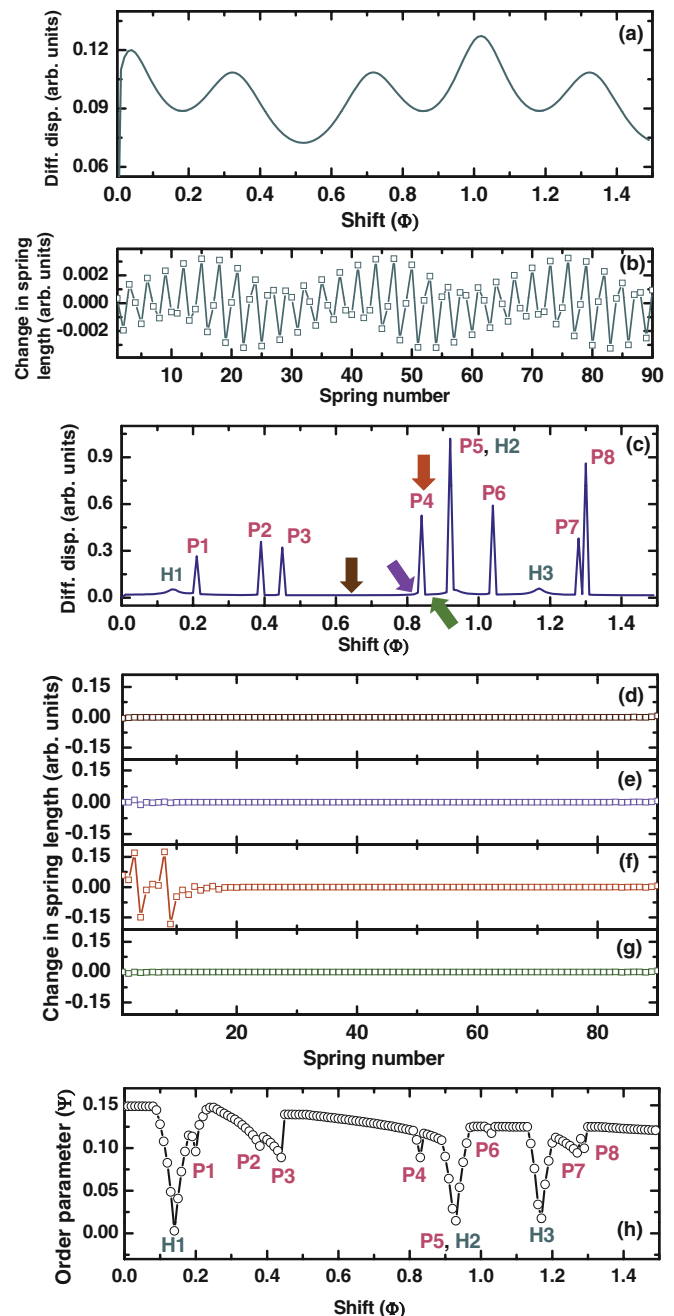


FIG. 2. (Color online) (a) Differential displacement and (b) change in the length of springs for the FK chain accommodating $N = 91$ particles in $N_v = 60$ valleys with $E/\kappa = 0.01$. (c) At $E/\kappa = 0.035$, the differential displacement profile shows intermittent relaxation bursts (P1–P8) along with three small humps (H1, H2, H3). (d)–(g) Changes in the lengths of the 90 springs showing the stick [(d),(e)] to slip [(f)] transition at peak P4, followed by another stick state [(g)] corresponding to the instants indicated by the four arrows in (c). (h) Variation in Ψ as a function of Φ . The features corresponding to the humps and peaks in (c) are marked here as well. The peaks in (c) always coincide with discontinuous jumps in Ψ .

lengths of the connecting springs in between two successive steps is shown in Fig. 2(b), where the change is noticed along the entire chain. With an increase in the value of E/κ , this

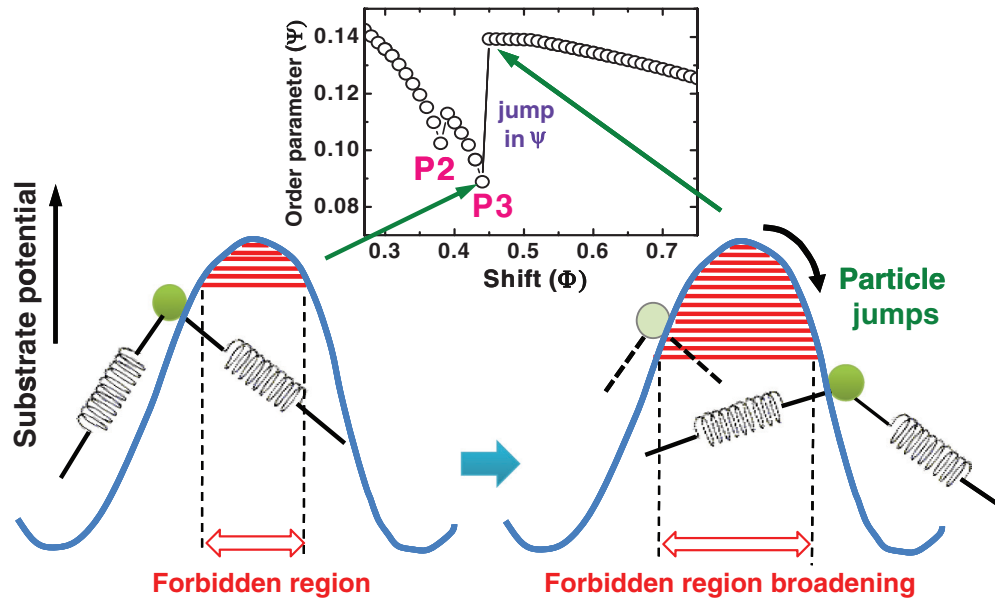


FIG. 3. (Color online) Schematic representation of discontinuous rise in the order parameter Ψ , as the sudden broadening of the forbidden region. This causes the particle in the FK chain to abruptly cross the potential hill.

wavy nature changes to relaxation bursts characterized by the intermittent peaks,²⁵ which can be seen from Fig. 2(c) for $E/\kappa = 0.035$. Remarkably, these peaks which demonstrate the phenomenon of quasistatic stick-slip are present here also, similar to those in Figs. 1(b)–1(e). Corresponding changes in the length of springs, which are confined to the regions near the fixed ends of the chain [Fig. 2(f)] are also intermittent and synchronized with the occurrence of relaxation bursts.²⁵

IV. GROUND STATE AND ORDER PARAMETER

For the FK chain in its ground state, the minimum distance of the particle from the nearest maximum of the substrate potential has been used as an order parameter by Coppersmith and Fisher²⁶ to characterize the Aubry-transition and breaking of analyticity.⁹ For the plot shown in Fig. 2(c), E/κ is large enough to cause the breaking of analyticity. However, in this study we encounter another variable Φ , denoting the extent of shift in the chain, which determines the ground state configuration of the entire chain. Therefore, the order parameter given by $\Psi = \min |x_i(\text{mod } 1) - 0.5|_{i \neq 1, N}$ has been computed and displayed in Fig. 2(h) as a function of Φ . A finite nonzero value of Ψ signifies the span of region around the top of the substrate potential where the presence of a particle is forbidden. It is noticeable that despite the apparently sudden occurrences of relaxation bursts, the instant of peak in Fig. 2(c) is always preceded by a gradual drop in Ψ [Fig. 2(h)] during the *stick* state, thereby indicating the gradual narrowing of the forbidden region. Thereafter a discontinuous jump in Ψ coincides with the transition to *slip* state at which the relaxation burst occurs.²⁵ This is indicative of abrupt broadening of the forbidden regions, and consequently, we expect at least one particle to suddenly cross over the peak of the substrate potential (see the schematic in Fig. 3) thereby causing a steep rise in the differential displacement profile. In addition, Fig. 2(h) also shows three instances where Ψ drops and reaches

values close to zero, and then rises continuously. Because of this continuous change in the order parameter, we observe small humps in the differential displacement profile which is in sharp contrast to the abrupt peaks, where the rise in Ψ is discontinuous. This can be somewhat difficult to identify, for example, during the second hump (H2), where it coincides with the occurrence of the fifth peak (P5) in the observed profile.

Typical ground state configurations of the FK chain are given in Fig. 4(a), where most of the particles follow a structural pattern associated with a highly stable energy state and attempt to maintain it despite the incremental change in Φ . As a result, the local configurations near the two fixed ends are out of skew with the rest of the chain, and the total energy of the system increases until the next relaxation burst. During this stick state the differential displacements of particles are found to be negligibly small, and hence, the coordinates of the particles, $x_i(\text{mod } 1)$ after relaxation, when plotted with respect to the coordinates before energy minimization show the linear behavior [Fig. 4(d)]. However, during a relaxation burst some of the coordinates are knocked out of the straight line pattern, as shown in Fig. 4(c). As predicted earlier, there is always one or more particles which cross the peak of the substrate potential corresponding to $x_i(\text{mod } 1) = 0.5$ as marked in the figure.²⁵

V. PRINCIPAL COMPONENT ANALYSIS

The FK chain presented here is a 1D model of an essentially 3D atomic structure of a dislocation in crystal. Each and every relaxation burst always drives the chain in a forward direction as both ends are shifted in the same direction. Similarly, it must be ascertained that the relaxation bursts as observed in the atomistic simulation of dislocation core also drive the core in an effectively forward direction. The notion of directionality is trivial in the FK model because of the inherent single dimensionality associated with the structure. However, the motion of a dislocation can be perceived only on a

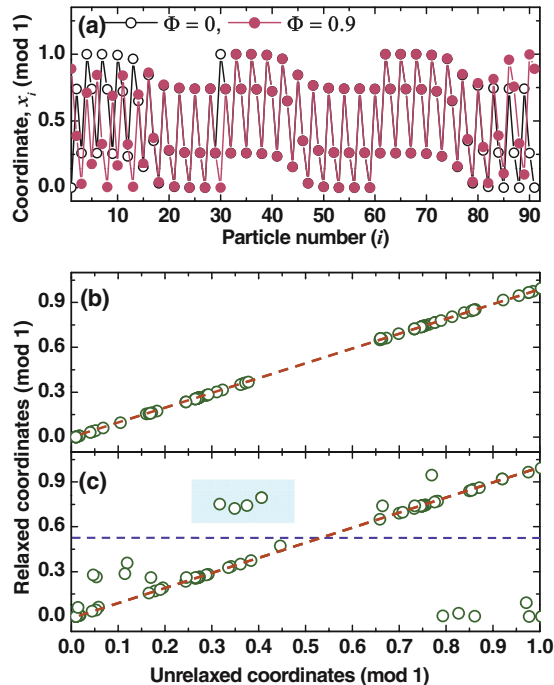


FIG. 4. (Color online) (a) Two typical ground state configurations of the FK chain ($\Phi = 0, 0.9$) with $N = 91$ particles in $N_v = 60$ valleys for $E/\kappa = 0.035$. The relaxed coordinates of the particles (b) just before and (c) at the instant of occurrence of the peak P5 in Fig. 2(c) plotted with respect to the unrelaxed coordinates. The particles which have crossed the maxima of the substrate potential, i.e., $x_i(\text{mod } 1) = 0.5$ (shown by dotted horizontal line), are identified in the rectangular frame.

coarse scale of length, where the dislocation hops from one lattice site to another. On a sub-Burgers vector scale of length, it is difficult to associate a sense of *unidirectional* motion to the self-assembly of core atoms within the same Peierls valley unless a specific directionality is ascribed to it. Clearly, the conventional technique of describing the core position as the center of mass of all the core atoms (Refs. 14, 27, and 28, for example) lacks the requisite resolution, and an alternative data mining tool needs to be explored. In this scenario, we opt to use the PCA¹⁸ as a prolific tool capable of providing a high degree of compressibility of high dimensional data and furnish its projection on a hyperspace of reduced effective dimensionality. The versatility of the PCA is reflected in its successful applications across a wide range of studies.^{29–33} In the present case of atomistic simulations, the coordinates of core atoms are recorded at each step of incremental shear strain and this strain series data is arranged as a $n_s \times 3n_c$ matrix, where n_s denotes the number of strain steps and n_c is the number of core atoms. Now each of the $3n_c$ columns is separately mean centered³⁴ and the mean-deviation matrix thus formed is used to generate the covariance matrix.¹⁸ Diagonalization of the covariance matrix yields the eigenvalues and the corresponding eigenvectors. Interestingly, for all the metals under study, the largest normalized eigenvalues are always found to be in excess of 90%. Such large values conclusively prove a high compressibility intrinsic to these sets of multidimensional data. The projections of the datasets along the principal directions corresponding to the largest

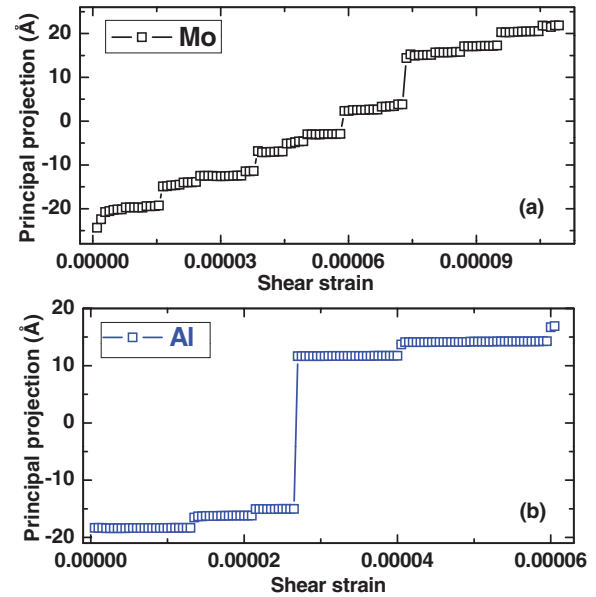


FIG. 5. (Color online) Principal projections for (a) molybdenum and (b) aluminium show staircaselike profiles. The quasiplateaus represent the stick states, whereas the slip states are reflected as the sudden jumps.

eigenvalues are presented in Fig. 5 for Mo and Al, for example. The sudden jumps present in these devil's staircaselike profiles are synchronized with the occurrence of peaks in Figs. 1(b) and 1(d) and are typical signatures of the stick-slip process (see the first and second panels of Fig. 4 in Ref. 6). Moreover, one can also observe that each monotonic jump in the projected profile always causes a translation in the same direction, thereby offering a ground for comparison with the FK model.

VI. CONCLUSION

To conclude, we have shown that the events of stick-slip, which are well known in the context of dynamic processes, can also be found during the quasistatic structural rearrangements of dislocation cores. Similar features are observed for the simple one-dimensional FK chain as well. This is attributed to a transition of the system from an effective stick to slip state on account of abrupt broadening of the forbidden region around the peak of the substrate potential. Furthermore, the projections of the atomic trajectories on the principle directions corroborate the efficacy of the one-dimensional FK chain in revealing the quasistatic behavior of a complex three-dimensional structure. However, one issue is yet to be resolved. Although the simplicity of the FK chain permits us to fathom the underlying mechanism of the stick-slip, it would be challenging to establish its direct link with a realistic system of interest, like the dislocation. As the FK chain has been used to model a large variety of physical systems besides dislocation cores, the quasistatic responses of other such systems merit further extensive investigations.

ACKNOWLEDGMENTS

A. Dutta acknowledges the financial support from CSIR, India to carry out this research work.

*mishreyee@vecc.gov.in

- ¹O. M. Braun, Nicola Manini, and Erio Tosatti, *Phys. Rev. Lett.* **110**, 085503 (2013).
- ²A. Benassi, A. Vanossi, G. E. Santoro, and E. Tosatti, *Phys. Rev. Lett.* **106**, 256102 (2011).
- ³O. M. Braun and J. Röder, *Phys. Rev. Lett.* **88**, 096102 (2002).
- ⁴T. B. Mitchell, J. J. Bollinger, W. M. Itano, and D. H. E. Dubin, *Phys. Rev. Lett.* **87**, 183001 (2001).
- ⁵I. Albert, P. Tegzes, B. Kahng, R. Albert, J. G. Sample, M. Pfeifer, A. L. Barabasi, T. Vicsek, and P. Schiffer, *Phys. Rev. Lett.* **84**, 5122 (2000).
- ⁶U. Bockelmann, B. Essevaz-Roulet, and F. Heslot, *Phys. Rev. Lett.* **79**, 4489 (1997).
- ⁷A. L. Demirel and S. Granick, *Phys. Rev. Lett.* **77**, 4330 (1996).
- ⁸Y. I. Frenkel and T. Kontorova, *Zh. Eksp. Teor. Fiz.* **8**, 1340 (1938) [*Sov. Phys. JETP* **13**, 1 (1938)].
- ⁹O. M. Braun and Y. S. Kivshar, *The Frenkel-Kontorova Model: Concepts, Methods, and Applications* (Springer-Verlag, New York, 2004).
- ¹⁰F.-J. Elmer, *Phys. Rev. E* **50**, 4470 (1994).
- ¹¹Z. Zheng, B. Hu, and G. Hu, *Phys. Rev. B* **58**, 5453 (1998).
- ¹²O. M. Braun, A. Vanossi, and E. Tosatti, *Phys. Rev. Lett.* **95**, 026102 (2005).
- ¹³R. E. Peierls, *Proc. Phys. Soc.* **52**, 34 (1940); F. R. N. Nabarro, *ibid.* **59**, 256 (1947).
- ¹⁴V. V. Bulatov and W. Cai, *Computer Simulations of Dislocations* (Oxford University Press, Oxford, 2006).
- ¹⁵D. L. Olmsted, K. Y. Hardikar, and R. Phillips, *Modelling Simul. Mater. Sci. Eng.* **9**, 215 (2001).
- ¹⁶R. E. Voskoboynikov, Yu. N. Osetsky, and D. J. Bacon, *Mater. Sci. Engg. A* **400–401**, 45 (2005).
- ¹⁷O. Braun *et al.*, *Physica D* **123**, 357 (1998).
- ¹⁸I. T. Jolliffe, *Principle Component Analysis* (Springer-Verlag, New York, 2002).
- ¹⁹The simulation reported here are performed using the MD++ code available at <http://micro.stanford.edu>.
- ²⁰J. P. Hirth and J. Lothe, *Theory of Dislocations* (John Wiley and Sons., New York, 1982).
- ²¹As there is no exact definition of the core region, the choice of the CSD window is empirical. However, the results presented here are not very sensitive to the choice of filtering windows so far as most of the core atoms are included.
- ²²M. W. Finnis and J. E. Sinclair, *Philos. Mag. A* **50**, 45 (1984); **53**, 161 (1986); G. J. Ackland and R. Thetford, *ibid.* **56**, 15 (1987).
- ²³F. Ercolessi and J. B. Adams, *Europhys. Lett.* **26**, 583 (1994).
- ²⁴S. M. Foiles, M. I. Baskes, and M. S. Daw, *Phys. Rev. B* **33**, 7983 (1986).
- ²⁵See Supplemental Material at <http://link.aps.org/supplemental/10.1103/PhysRevB.87.214107> for the movie clips for differential displacements, change in the lengths of springs, order parameter, ground state configuration, and relaxed vs unrelaxed coordinates.
- ²⁶S. N. Coppersmith and D. S. Fisher, *Phys. Rev. B* **28**, 2566 (1983).
- ²⁷A. Dutta, M. Bhattacharya, P. Barat, P. Mukherjee, N. Gayathri, and G. C. Das, *Phys. Rev. Lett.* **101**, 115506 (2008).
- ²⁸M. Bhattacharya, A. Dutta, P. Mukherjee, N. Gayathri, and P. Barat, *Phys. Rev. B* **82**, 184113 (2010).
- ²⁹K. I. Kim, M. O. Franz, and B. Schölkopf, *IEEE Trans. Pattern Analysis and Machine Intell.* **27**, 1351 (2005).
- ³⁰M. S. Wagner and D. G. Castner, *Langmuir* **17**, 4649 (2001).
- ³¹J. Hasbrouck and D. J. Seppi, *J. Financial Econ.* **59**, 383 (2001).
- ³²I. Vaquila, M. C. G. Passeggi, and J. Ferrón, *Phys. Rev. B* **55**, 13925 (1997).
- ³³S. V. Kalinin, B. J. Rodriguez, J. D. Budai, S. Jesse, A. N. Morozovska, A. A. Bokov, and Z. G. Ye, *Phys. Rev. B* **81**, 064107 (2010).
- ³⁴In the present study, we have actually made use of the so-called “conditioned” data, which means that the data is not only mean centered, but scaled so as to normalize the variances as well. Although PCA would work only with mean centering also, complete conditioning is often prescribed as a better way of preprocessing the data.